Influence of dynamic tortuosity and compressibility on the propagation of transient waves in porous media

Zine El Abiddine E.A. Fellah, Claude Depollier, Mohamed Fellah, Walter Lauriks, Jean-Yves Chapelon

Influence of dynamic tortuosity and compressibility on the propagation of transient waves in porous media

Z.E.A. Fellah [a,*], C. Depollier [b], M. Fellah [c], W. Lauriks [d], J.-Y. Chapelon [a]

[a] *National Institute of Health and Medical Research (INSERM U556), 151 cours Albert Thomas, 69424 Lyon Cedex 03, France*
[b] *Laboratoire d'Acoustique de l'Université du Maine, UMR-CNRS 6613, Université du Maine, Avenue Olivier Messiaen 72085 Le Mans Cedex 09, France*
[c] *Laboratoire de Physique Théorique, Institut de Physique, USTHB, BP 32 El Alia, Bab Ezzouar 16111, Algeria*
[d] *Laboratorium voor Akoestiek en Thermische Fysica, Katholieke, Universiteit Leuven, Celestijnenlaan 200 D, B-3001 Heverlee, Belgium*

This paper provides an analytical solution in the time domain for the propagation of transient ultrasonic waves in a homogeneous, isotropic porous material with a rigid frame. The originality of this propagation equation is the use of the Pride et al. and Lafarge models, which give a better description of acoustic wave attenuation. Two parameters, p and p', are added to the description of losses in the porous material, given a modification of coefficients of the propagation equation in the time domain. The analytical solution to the wave equation has a different form as compared with that obtained from the Johnson–Allard model. This wave equation contains fractional derivative terms describing attenuation and dispersion in porous material. The Laplace transform method is used to solve the propagation equation. An experimental application to porous plastic foam is given to validate the mathematical solution to the propagation equation.

One important result of this work is that the introduction of the two parameters p and p' corrects the Johnson–Allard model by increasing attenuation with no change in dispersion. This phenomenon is much more significant for resistive porous materials.

Keywords: Pulse propagation; Transient signals; Porous material

1. Introduction

Porous media filled with air, such as fibrous mats, plastic foams and various felts, are used intensively in the automobile, aeronautical and building industries to attenuate sound waves. In the recent past, low frequency (i.e. in the range of 20–600 kHz) ultrasonic techniques have amply proven their worth as a powerful tool for probing the acoustic properties of these materials.

The geometry of the pores in ordinary porous media is not simple, and it is not easy to calculate the viscous and thermal interaction between fluid and structure directly. Useful information can be obtained from the simple case of porous materials with cylindrical pores. The Kirchhoff theory [1] of sound propagation in cylindrical tubes provides a general description of viscous and thermal effects, but this description is unnecessarily complicated for many

* Corresponding author. Tel.: +33-4-72-68-19-40; fax: +33-4-72-68-19-31.
E-mail address: fellah@lyon.inserm.fr (Z.E.A. Fellah).

applications. Moreover, the fundamental acoustics equations used in the Kirchhoff theory can be very difficult to solve in the case of a non-circular cross-section. A simplified model in which thermal and viscous effects are treated separately has been developed by Zwikker and Kosten [2] for the case of circular cross-sections. The validity of this model was later justified [3,4], for a range of radii from 10^{-3} cm to several centimeters at acoustic frequencies. This model was used to describe viscous effects in slits and cylindrical tubes with a circular cross-section. Thermal exchange effects were related to viscous effects using a model developed by Stinson [4]. For common porous materials, it is generally impossible to model the bulk modulus and effective mass forming the frame geometry. This explains why the models that describe sound propagation in these materials are mostly phenomenological. A review of the models developed before 1980 can be found in a work by Attenborough [5]. More recent studies have been performed by Lambert [6] and Attenborough [7].

In 1987, a substantial contribution was made by Johnson et al. [8], who released a theory of dynamic fluid flow (i.e. as a function of frequency) in porous media, introducing the concept of dynamic tortuosity and permeability as well as viscous characteristics and length. Originally, the research mainly focussed on geophysical and petroleum industry applications. The Johnson et al. model was used for different kinds of porous materials [9–13]. For gas-saturated porous media, Allard [9] has produced an analogous theory for thermal effects, by introducing the concept of thermal characteristic length. Lafarge et al. [14,15] have extended this theory by adding the concept of thermal permeability which plays an important part at low frequency approximation.

To cope efficiently with the specific problems appearing in transient acoustic field propagation, new approaches are required [16]. At present, most analyses of signal propagation are carried out in the frequency domain using the Fourier transform, and the results are translated to the time domain, and vice-versa. However this has several limitations. The first one is that the transformation is difficult to compute numerically with sufficient accuracy for non-analytical functions. For example, using the Fourier transform to obtain time domain results for a lossy material is a more complicated approach than using a true time domain analysis, and the numerical results are less accurate. The second disadvantage is that by working in the frequency domain, some numerical information is lost or hard to recover. For example, in the case of noisy data it may be difficult to reconstruct the chronological events of a signal by phase unwrapping. Consequently, it is difficult to obtain a deep understanding of transient signal propagation using the frequency domain method.

In our previous paper [13] we analytically calculated the solution in the time domain for the propagation of transient ultrasonic waves in a homogeneous isotropic porous material with a rigid frame, using the Johnson et al. [8] and Allard [9] model. However Pride et al. [17] and Lafarge [15] show that the Johnson et al. [8] and Allard [9] model underestimates the imaginary part of the relaxation functions of the porous medium. This underestimation affects attenuation of the ultrasonic pulse and then the physical parameters estimated by the inverse problem. In this work, a general analytical solution in the time domain is proposed, in which the Pride et al. [17] and Lafarge [15] models are taken into account. This solution has been validated by experimental data.

2. Model

In the acoustics of porous materials, a distinction can be made between two situations depending on whether the frame is deformable or not. In the first alternative, the dynamics of the waves due to coupling between the solid frame and the fluid are clearly described by the Biot theory [18,19]. In air-saturated porous media, the structure is generally motionless and the waves propagate only in the fluid. This case is described by the equivalent fluid model, which is a particular instance of the Biot model.

Let a homogeneous isotropic porous material with porosity ϕ be saturated with a compressible and viscous fluid of density ρ_f and viscosity η. It is assumed that the frame of this porous solid is not deformable when subjected to an acoustic wave. This is the case, for example for a porous medium with high skeleton density or a very large elastic modulus or weak fluid-structure coupling. To apply the results of continuum mechanics the wave-length of sound must be much larger than the sizes of the pores or grains in the medium.

In such porous material, acoustic waves propagate only in the fluid, so it can be seen as an equivalent fluid, the density and bulk modulus of which are "renormalized" by fluid-structure interactions. A prediction of the acoustic behavior of the porous material requires the dynamic tortuosity $\alpha(\omega)$ and the dynamic compressibility $\beta(\omega)$ to be determined. These functions depend on the physical characteristics of the fluid in the pore space of the medium and are independent of the dynamic characteristics of the structure. The basic equations of the equivalent fluid model are given in frequency domain [9] by

$$\rho_{\mathrm{f}}\alpha(\omega)\mathrm{i}\omega v_i = \nabla_i p, \qquad \frac{\beta(\omega)}{K_a}\mathrm{i}\omega = \nabla \cdot v. \tag{1}$$

In these relations, v and p are the particle velocity and acoustic pressure, $K_a = \gamma P_0$ is the compressibility modulus of the fluid. The first equation is the Euler equation, and the second one is a constitutive equation. $\alpha(\omega)$ and $\beta(\omega)$ are the dynamic tortuosity of the medium and the dynamic compressibility of the air in the porous material. These two factors are complex functions which depend heavily on the frequency $f = \omega/2\pi$. Their theoretical expressions are given by Johnson et al. [8], Allard [9] and Lafarge [14]

$$\alpha(\omega) = \alpha_\infty \left(1 - \frac{\eta\phi}{\mathrm{i}\omega\alpha_\infty\rho_{\mathrm{f}}k_0}\sqrt{1 - \mathrm{i}\frac{4\alpha_\infty^2 k_0^2\rho_{\mathrm{f}}\omega}{\eta\Lambda^2\phi^2}}\right), \tag{2}$$

$$\beta(\omega) = \gamma - (\gamma-1)\left(1 - \frac{\eta\phi}{\mathrm{i}\omega\rho_{\mathrm{f}}k_0' Pr}\sqrt{1 - \mathrm{i}\frac{4k_0'^2\rho_{\mathrm{f}}\omega Pr}{\eta\phi^2\Lambda'^2}}\right)^{-1}, \tag{3}$$

where $\mathrm{i}^2 = -1$, γ represents the adiabatic constant, Pr the Prandtl number, α_∞ the tortuosity, η is fluid viscosity, k_0 viscous permeability, k_0' thermal permeability [14], Λ and Λ' viscous and thermal characteristic lengths [8,9]. This model was initially developed by Johnson [8], and completed by Allard [9] by adding the description of thermal effects. Later on, Lafarge [14] introduced the parameter k_0' which describes the additional damping of sound waves due to thermal exchanges between fluid and structure at the surface of the pores.

The functions $\alpha(\omega)$ and $\beta(\omega)$ express the viscous and thermal exchanges between the air and the structure which are responsible for sound damping in acoustic materials. These exchanges are due, on the one hand, to relative fluid-structure motion and, on the other hand, to air compression-dilatations produced by the wave motion. The parts of the fluid affected by these exchanges can be estimated by the ratio of a microscopic characteristic length of the media, for example pore size, to viscous and thermal skin depth thickness $\delta = (2\eta/\omega\rho_0)^{1/2}$ and $\delta' = (2\eta/\omega\rho_0 Pr)^{1/2}$. For viscous effects, this domain corresponds to the region of the fluid in which the velocity distribution is disturbed by frictional forces at the interface between the viscous fluid and the motionless structure. For thermal effects, it corresponds to the fluid volume affected by heat exchange between the two phases of the porous medium. In this model, sound propagation is completely determined by the following six parameters: ϕ, α_∞, $\sigma = \eta/k_0$ (flow resistivity), k_0', Λ and Λ'.

An underestimation of the imaginary part of the relaxation functions $\alpha(\omega)$ and $\beta(\omega)$ was corrected by Pride et al. [17] and Lafarge [15] by adding two geometrical parameters p and p'. The authors [15,17] suggest the following expressions of dynamic tortuosity and compressibility

$$\alpha(\omega) = \alpha_\infty \left(1 - \frac{\eta\phi}{\mathrm{i}\omega\alpha_\infty\rho_{\mathrm{f}}k_0}\left(1 - p + p\sqrt{1 - \mathrm{i}\frac{2\alpha_\infty^2 k_0^2\rho_{\mathrm{f}}\omega}{\eta\Lambda^2\phi^2 p^2}}\right)\right), \tag{4}$$

$$\beta(\omega) = \gamma - (\gamma-1)\left(1 - \frac{\eta\phi}{\mathrm{i}\omega\rho_{\mathrm{f}}k_0' Pr}\left(1 - p' + p'\sqrt{1 - \mathrm{i}\frac{2k_0'^2\rho_{\mathrm{f}}\omega Pr}{\eta\phi^2\Lambda'^2 p'^2}}\right)\right)^{-1}. \tag{5}$$

It can be seen that for $p = p' = 1$, the Pride–Lafarge model reduces to the Johnson–Allard model. Some values of parameters p and p' have been calculated by Lafarge for particular pore geometry [15].

3. Asymptotic domain

The asymptotic domain is defined when the viscous effects are concentrated within a small volume near the frame and the compression/dilation cycle is faster than the heat transfer between the air and the structure, and it is a good approximation to consider that compression is adiabatic.

This domain corresponds to the range of frequencies such that viscous skin thickness $\delta = (2\eta/\omega\rho_0)^{1/2}$ is smaller than pore radius r, and corresponds to a high-frequency approximation of the response factors $\alpha(\omega)$ and $\beta(\omega)$ when $\omega \to \infty$, their expressions are given by

$$\alpha(\omega) = \alpha_\infty \left(1 + \frac{2}{\Lambda}\left(\frac{\eta}{-\mathrm{i}\omega\rho_\mathrm{f}}\right)^{1/2} - \frac{\sigma\phi(1-p)}{\mathrm{i}\omega\rho_\mathrm{f}\alpha_\infty}\right), \tag{6}$$

$$\beta(\omega) = 1 + (\gamma - 1)\left(\frac{2}{\Lambda'}\left(\frac{\eta}{-\mathrm{i}\omega Pr\rho_\mathrm{f}}\right)^{1/2} - \frac{\eta\phi(1-p')}{\mathrm{i}\omega k_0' Pr\rho_\mathrm{f}}\right). \tag{7}$$

In the time domain, $\alpha(\omega)$ and $\beta(\omega)$ are expressed by the temporal operators $\tilde{\alpha}(t)$ and $\tilde{\beta}(t)$

$$\tilde{\alpha}(t) = \alpha_\infty \left(\delta(t) + \frac{2}{\Lambda}\left(\frac{\eta}{\rho_\mathrm{f}}\right)^{1/2} \frac{\partial^{-1/2}}{\partial t^{-1/2}} + \frac{\sigma\phi(1-p)}{\rho_\mathrm{f}\alpha_\infty}\frac{\partial^{-1}}{\partial t^{-1}}\right), \tag{8}$$

$$\tilde{\beta}(t) = \delta(t) + (\gamma - 1)\left(\frac{2}{\Lambda'}\left(\frac{\eta}{Pr\rho_\mathrm{f}}\right)^{1/2} \frac{\partial^{-1/2}}{\partial t^{-1/2}} + \frac{\eta\phi(1-p')}{k_0' Pr\rho_\mathrm{f}}\frac{\partial^{-1}}{\partial t^{-1}}\right). \tag{9}$$

In these equations, $\delta(t)$ is the Dirac delta function, the temporal operator $\partial^{-1}/\partial t^{-1}$ represents an Integral

$$\frac{\partial^{-1}x(t)}{\partial t^{-1}} = \int_0^t x(t')\,\mathrm{d}t',$$

and the semi integral operator $\partial^{-1/2}/\partial t^{-1/2}$ is given by the following definition of the fractional integrals of order ν given in Samko et al. [20]

$$D^\nu[x(t)] = \frac{1}{\Gamma(-\nu)}\int_0^t (t-u)^{-\nu-1}x(u)\,\mathrm{d}u, \tag{10}$$

where $\Gamma(x)$ is the gamma function.

In this framework, the basic equation (1) of this model can be expressed as follows:

$$\rho_\mathrm{f}\tilde{\alpha}(t) * \frac{\partial v_i}{\partial t} = -\nabla_i p \quad \text{and} \quad \frac{\tilde{\beta}(t)}{K_a} * \frac{\partial p}{\partial t} = -\nabla\cdot v, \tag{11}$$

where $*$ denotes the time convolution operation. For a wave propagating along the x-axis, using (8) and (9), one finds that Eq. (11) yields

$$\rho_\mathrm{f}\alpha_\infty\frac{\partial v(x,t)}{\partial t} + 2\frac{\rho_\mathrm{f}\alpha_\infty}{\Lambda}\left(\frac{\eta}{\pi\rho_\mathrm{f}}\right)^{1/2}\int_0^t \frac{\partial v(x,t)/\partial t'}{\sqrt{t-t'}}\,\mathrm{d}t' + \sigma\phi(1-p)\cdot v(x,t) = -\frac{\partial p(x,t)}{\partial x}, \tag{12}$$

$$\frac{1}{K_a}\frac{\partial p(x,t)}{\partial t} + 2\frac{\gamma-1}{K_a\Lambda'}\left(\frac{\eta}{\pi Pr\rho_\mathrm{f}}\right)^{1/2}\int_0^t \frac{\partial p(x,t)/\partial t'}{\sqrt{t-t'}}\,\mathrm{d}t' + \frac{(\gamma-1)\eta\phi(1-p')}{k_0' Pr\rho_\mathrm{f}}p(x,t) = -\frac{\partial v(x,t)}{\partial x}. \tag{13}$$

In these equations, the convolutions express the dispersive nature of the porous material. They take into account the memory effects, where the response of the medium to the wave excitation is not instantaneous but needs some time to take effect.

4. Direct problem

The direct scattering problem is that of determining the scattered field as well as the internal field, that arises when a known incident field impinges on the porous material with known physical properties. To compute the solution of the direct problem one need to know the Green's function of the modified wave equation in the porous medium. In that case, the internal field is given by the time convolution of the Green's function with the incident wave and the reflected and transmitted fields are deduced from the internal field and the boundary conditions.

The generalized lossy wave equation in the time domain is derived from the basic equations (12) and (13) by elementary calculation in the following form

$$\frac{\partial^2 p(x,t)}{\partial x^2} - A\frac{\partial^2 p(x,t)}{\partial t^2} - B\int_0^t \frac{\partial^2 p(x,t)/\partial t'^2}{\sqrt{t-t'}}\,\mathrm{d}t' - C\frac{\partial p(x,t)}{\partial t} = 0, \tag{14}$$

where coefficients A, B and C are constants expressed by

$$A = \frac{1}{c^2} = \frac{\rho_\mathrm{f}\alpha_\infty}{K_a}, \qquad B = \frac{2\alpha_\infty}{K_a}\sqrt{\frac{\rho_\mathrm{f}\eta}{\pi}}\left(\frac{1}{\Lambda} + \frac{\gamma-1}{\sqrt{Pr}\Lambda'}\right), \tag{15}$$

$$C = \left(\frac{4\alpha_\infty(\gamma-1)\eta}{K_a\Lambda\Lambda'\sqrt{Pr}} + \frac{\sigma\phi(1-p)}{K_a} + \frac{\alpha_\infty(\gamma-1)\eta\phi(1-p')}{K_a k_0' Pr}\right). \tag{16}$$

The first one is related to the velocity $c = 1/\sqrt{\rho_\mathrm{f}\alpha_\infty/K_a}$ of the wave in the air contained within the porous material. The coefficient α_∞ is the refractive index of the medium that changes wave velocity from $c_0 = \sqrt{K_a/\rho_\mathrm{f}}$ in free space to $c = c_0/\sqrt{\alpha_\infty}$ in the porous medium. The other coefficients are essentially dependent on the characteristic lengths Λ and Λ', and the two new parameters p and p' introduced by the Pride et al. and Lafarge models, and express the viscous and thermal interactions between the fluid and the structure. Coefficients A and B are the same in both the Johnson–Allard model and Pride–Lafarge models, but parameter C has been modified by the introduction of parameters p and p'. We will see in the next section how modification of the coefficient C can considerably change the analytical solution in the time domain of this Eq. (14).

4.1. Reflection and transmission scattering operators

Consider a homogeneous porous medium which fills the region $0 \le x \le L$. This medium is assumed to be isotropic and to have a rigid frame. A short sound pulse impinges normally on the medium from the left. It gives rise to an acoustic pressure field $p(x,t)$ and an acoustic velocity field $v(x,t)$ within the material, which satisfying the propagation Eq. (14) written also as:

$$\frac{\partial^2 p(x,t)}{\partial x^2} - \left(\frac{1}{c^2}\delta(t) + CH(t) + \frac{B}{\sqrt{t}}\right) * \frac{\partial^2 p(x,t)}{\partial t^2} = C\frac{\partial p}{\partial t}(x,0), \tag{17}$$

where $H(t)$ is the Heaviside function: $H(t) = 0$ for $t \le 0$ and $H(t) = 1$, for $t > 0$.

To derive the reflection and transmission scattering operators, it is assumed that the pressure field and flow velocity are continuous at the material boundary.

$$p(0^+,t) = p(0^-,t), \qquad p(L^-,t) = p(L^+,t), \qquad v(0^-,t) = \phi v(0^+,t), \qquad v(L^+,t) = \phi v(L^-,t), \tag{18}$$

where ϕ is the porosity of the medium and $\pm$ superscript denotes the limit from left and right, respectively. Assumed initial conditions are:

$$p(x,t)|_{t=0} = 0 \quad \text{and} \quad \left.\frac{\partial p}{\partial t}\right|_{t=0} = 0, \tag{19}$$

which means that the medium is idle for $t = 0$.

If the incident sound wave is generated in region $x \leq 0$, then the expression of the acoustic field in the region to the left of the material is the sum of the incident and reflected fields

$$p_1(x,t) = p^{\mathrm{i}}\left(t - \frac{x}{c_0}\right) + p^{\mathrm{r}}\left(t + \frac{x}{c_0}\right), \quad x < 0, \tag{20}$$

here, $p_1(x,t)$ is the field in region $x < 0$, p^{i} and p^{r} denotes the incident and reflected fields respectively. In addition, a transmitted field is produced in the region to the right of the material. This has the form

$$p_3(x,t) = p^{\mathrm{t}}\left(t - \frac{L}{c} - \frac{(x-L)}{c_0}\right), \quad x > L. \tag{21}$$

($p_3(x,t)$ is the field in region $x > L$ and p^{t} is the transmitted field.)

The incident and scattered fields are related by scattering operators (i.e. reflection and transmission operators) for the material. These are integral operators represented by

$$p^{\mathrm{r}}(x,t) = \int_0^t \tilde{R}(\tau) p^{\mathrm{i}}\left(t - \tau + \frac{x}{c_0}\right) \mathrm{d}\tau = \tilde{R}(t) * p^{\mathrm{i}}(t) * \delta\left(t + \frac{x}{c_0}\right). \tag{22}$$

$$p^{t}(x,t) = \int_0^t \tilde{T}(\tau) p^{\mathrm{i}}\left(t - \tau - \frac{L}{c} - \frac{(x-L)}{c_0}\right) \mathrm{d}\tau = \tilde{T}(t) * p^{\mathrm{i}}(t) * \delta\left(t - \frac{L}{c} - \frac{(x-L)}{c_0}\right). \tag{23}$$

In Eqs. (22) and (23) functions $\tilde{R}$ and $\tilde{T}$ are the reflection and transmission kernels, respectively, for incidence from the left. Note that the lower limit of integration in (22) and (23) is given as 0, which is equivalent to assuming that the incident wave front first impinges on the material at $t = 0$. The operators $\tilde{R}$ and $\tilde{T}$ are independent of the incident field used in the scattering experiment and depend only on the properties of the materials.

Using boundary and initial conditions (18) and (19), reflection and transmission scattering operators can be derived [12], taking into account the n-multiple reflections in the material:

$$\tilde{R}(t) = \left(\frac{1-E}{1+E}\right) \sum_{n \geq 0} \left(\frac{1-E}{1+E}\right)^{2n} \left[G\left(t, 2n\frac{L}{c}\right) - G\left(t, (2n+2)\frac{L}{c}\right)\right], \tag{24}$$

$$\tilde{T}(t) = \frac{4E}{(1+E)^2} \sum_{n \geq 0} \left(\frac{1-E}{1+E}\right)^{2n} G\left(t + \frac{L}{c_0}, (2n+1)\frac{L}{c}\right). \tag{25}$$

In these equations, $E = \phi/\sqrt{\alpha_\infty}$ and G is the medium's Green function.

The solution $p(x,t)$ of the propagation equation (14) is given by the convolution of the Green function $G(x,t)$ with the input signal $p(0,t)$,

$$p(x,t) = \int_0^t G(t - t', x) p(0, t') \, \mathrm{d}t'. \tag{26}$$

In most cases of air-saturated porous materials, multiple reflection effects may be negligible because of the high attenuation of sound waves in these media. So, by taking into account only the first reflections at interfaces $x = 0$ and $x = L$, the expressions of the reflection and transmission operators will be given by

$$\tilde{R}(t) = \frac{\sqrt{\alpha_\infty} - \phi}{\sqrt{\alpha_\infty} + \phi} \delta(t) - \frac{4\phi\sqrt{\alpha_\infty}(\sqrt{\alpha_\infty} - \phi)}{(\sqrt{\alpha_\infty} + \phi)^3} G\left(t, \frac{2L}{c}\right), \tag{27}$$

$$\tilde{T}(t) = \frac{4\phi\sqrt{\alpha_\infty}}{(\phi+\sqrt{\alpha_\infty})^2} G\left(t + \frac{L}{c}, \frac{L}{c}\right). \tag{28}$$

4.2. General solution of the propagation equation

In order to obtain the Green function of the medium, we will solve Eq. (17) using the Laplace transform method [21,22], taking into account the conditions (19). We note $P(x, z)$ the Laplace transform of $p(x, t)$ defined by:

$$P(x, z) = \mathcal{L}[p(x, t)] = \int_0^\infty \exp(-zt)\, p(x, t)\, \mathrm{d}t, \tag{29}$$

and the inverse Laplace transform [21] by

$$p(x, t) = \mathcal{L}^{-1}[P(x, z)]. \tag{30}$$

Using the following relations

$$\mathcal{L}[\delta(t)] = 1, \qquad \mathcal{L}[H(t)] = \frac{1}{z} \quad \text{and} \quad \mathcal{L}\left[\frac{1}{\sqrt{t}}\right] = \sqrt{\frac{\pi}{z}}, \tag{31}$$

the Laplace transform of the wave Eq. (17) yields

$$\frac{\partial^2 P(x, z)}{\partial x^2} - z^2\left(\frac{1}{c^2} + \frac{C}{z} + B\sqrt{\frac{\pi}{z}}\right) P(x, z) = -\left(\frac{1}{c^2} + B\sqrt{\frac{\pi}{z}}\right)\left(zp(x, 0) + \frac{\partial p(x, 0)}{\partial t}\right) - Cp(x, 0). \tag{32}$$

Taking into account the initial conditions (19), Eq. (32) is simplified to

$$\frac{\partial^2 P(x, z)}{\partial x^2} - z^2\left(\frac{1}{c^2} + \frac{C}{z} + B\sqrt{\frac{\pi}{z}}\right) P(x, z) = 0, \tag{33}$$

which is a second-order differential equation with real constant coefficients. The characteristic equation of (33) is

$$r^2 - z^2\left(\frac{1}{c^2} + \frac{C}{z} + B\sqrt{\frac{\pi}{z}}\right) = 0. \tag{34}$$

The general solution of (23) has the form

$$P(x, z) = \mathrm{e}^{-x/c\sqrt{f(z)}}\varphi(z) + \mathrm{e}^{x/c\sqrt{f(z)}}\psi(z), \tag{35}$$

where $\varphi(z)$ and $\psi(z)$ are two functions independent of x and

$$f(z) = z^2\left(1 + \frac{Cc^2}{z} + Bc^2\sqrt{\frac{\pi}{z}}\right) = z^2 + Bc^2\sqrt{\pi}z\sqrt{z} + Czc^2 = z(z + b'\sqrt{z} + c'). \tag{36}$$

In Eq. (26), constants b' and c' are positive and are given by

$$b' = Bc^2\sqrt{\pi} \quad \text{and} \quad c' = Cc^2. \tag{37}$$

By taking the finite solution at infinity, which corresponds to the physical solution of our problem

$$P(x, z) = \mathrm{e}^{-x/c\sqrt{f(z)}}\varphi(z). \tag{38}$$

The solution of Eq. (17) is the inverse Laplace transform of $P(x, z)$. Thereby giving

$$p(x, t) = \mathcal{L}^{-1}(\mathrm{e}^{-x/c\sqrt{f(z)}}\varphi(z)) = \mathcal{L}^{-1}(\mathrm{e}^{-x/c\sqrt{f(z)}}) * \mathcal{L}^{-1}(\varphi(z)). \tag{39}$$

In the next section, we will calculate the term $\mathcal{L}^{-1}(\mathrm{e}^{-x/c\sqrt{f(z)}})$ which is the core of the problem.

4.3. Calculation of $\mathcal{L}^{-1}(\mathrm{e}^{-x/c\sqrt{f(z)}})$

By putting $\Delta^2 = b'^2 - 4c'$, it is easy to verify that Δ^2 is always positive when $p = p' = 1$, which is equivalent to the case of the Johnson–Allard model [13].

When $\Delta = 0$, the solution of the propagation Eq. (14) is given in Ref. [13] by

$$p(x,t) = \begin{cases} 0 & \text{if} \quad 0 \le t \le \dfrac{x}{c}, \\ \dfrac{1}{4\sqrt{\pi}} \dfrac{b'x}{c} \displaystyle\int_{x/c}^{t} \frac{1}{(\tau - x/c)^{3/2}} \exp\left(-\frac{b'^2x^2}{16c^2(\tau - x/c)}\right) p(0, t-\tau)\,\mathrm{d}\tau & \text{if} \quad t > \dfrac{x}{c}, \end{cases} \tag{40}$$

where $p(0,t) = \mathcal{L}^{-1}(\varphi(z))$. In this case, the Green function is given by

$$G(x,t) = \begin{cases} 0 & \text{if} \quad 0 \le t \le \dfrac{x}{c}, \\ \dfrac{1}{4\sqrt{\pi}} \dfrac{b'x}{c} \dfrac{1}{(t - x/c)^{3/2}} \exp\left(-\dfrac{b'^2x^2}{16c^2(t - x/c)}\right) & \text{if} \quad t > \dfrac{x}{c} \end{cases} \tag{41}$$

When $\Delta^2 > 0$, the general solution of the propagation Eq. (14) is given in Ref. [13] by

$$p(x,t) = \begin{cases} 0 & \text{if} \quad 0 \le t \le \dfrac{x}{c}, \\ \dfrac{x}{c} \displaystyle\int_{x/c}^{t} \left(\frac{b'}{4\sqrt{\pi}} \frac{1}{(\tau - x/c)^{3/2}} \exp\left(-\frac{b'^2x^2}{16c^2(\tau - x/c)}\right) + \Delta \int_0^{\tau - x/c} h'(\xi)\,\mathrm{d}\xi \right) p(0, t-\tau)\,\mathrm{d}\tau & \text{if} \quad t > \dfrac{x}{c}. \end{cases} \tag{42}$$

where

$$h'(\xi) = -\frac{1}{4\pi^{3/2}} \frac{1}{\sqrt{(\tau-\xi)^2 - x^2/c^2}} \frac{1}{\xi^{3/2}} \int_{-1}^{1} \exp\left(-\frac{(\mu\Delta\sqrt{(\tau-\xi)^2 - x^2/c^2} + b'(\tau-\xi))^2}{16\xi}\right) \times \left(\frac{(\mu\Delta\sqrt{(\tau-\xi)^2 - x^2/c^2} + b'(\tau-\xi))^2}{8\xi} - 1\right) \frac{\mu\,\mathrm{d}\mu}{\sqrt{1-\mu^2}}. \tag{43}$$

In this case, the Green function is given by

$$G(x,t) = \begin{cases} 0 & \text{if} \quad 0 \le t \le \dfrac{x}{c}, \\ \dfrac{x}{c} \left(\dfrac{b'}{4\sqrt{\pi}} \dfrac{1}{(t - x/c)^{3/2}} \exp\left(-\dfrac{b'^2x^2}{16c^2(t - x/c)}\right) + \Delta \displaystyle\int_0^{t - x/c} h'(\xi)\,\mathrm{d}\xi \right) & \text{if} \quad t > \dfrac{x}{c}. \end{cases} \tag{44}$$

For the Pride–Lafarge model, Δ^2 can be negative. This is because the value of the coefficient C in the propagation Eq. (14) is modified by introducing the parameters p and p'. We will now consider the general solution of the propagation Eq. (14) by considering the Pride–Lafarge model and thus by considering the case where Δ^2 is negative.

4.3.1. Case when $\Delta^2 < 0$

Let be

$$\Delta'^2 = -\Delta^2 \Rightarrow \Delta'^2 = 4c' - b'^2. \tag{45}$$

In this case, $f(z)$ can be put in the following form

$$f(z) = \left(z + \frac{b'}{2}\sqrt{z}\right)^2 + \left(\frac{\Delta'\sqrt{z}}{2}\right)^2. \tag{46}$$

Using Eqs. (45) and (46) and the analytical calculus given in Appendix A, we obtain the solution of the propagation Eq. (14) when Δ^2 is negative

$$p(x,t) = \begin{cases} 0 & \text{if} \quad 0 \le t \le \dfrac{x}{c}, \\ \int_{x/c}^{t} \left[F_1(\tau) + \int_0^{\tau - x/c} H(\xi,\tau)\,\mathrm{d}\xi + i \int_0^{\tau - x/c} \Xi(\xi,\tau)\,\mathrm{d}\xi \right] p(0, t-\tau)\,\mathrm{d}\tau & \text{if} \quad t > \dfrac{x}{c}. \end{cases} \tag{47}$$

with

$$F_1(\tau) = \frac{1}{4\sqrt{\pi}} b' \frac{x}{c} \frac{1}{(\tau - x/c)^{3/2}} \exp\left(-\frac{b'^2 x^2}{16(\tau - x/c)} \right).$$

The functions $H(\xi,\tau)$ and $\Xi(\xi,\tau)$ are given by the following relations in which, t is replaced by τ:

$$H(\xi,t) = \frac{\Delta'}{4\pi\sqrt{\pi}} \frac{x}{c} \frac{1}{\sqrt{(t-\xi)^2 - x^2/c^2}} \frac{1}{\xi^{3/2}} \int_{-1}^{1} \left[\frac{\mathcal{A}\mathcal{B}}{4\xi} \cos\left(\frac{\mathcal{A}\mathcal{B}}{8\xi}\right) - \left(\frac{\mathcal{B}^2 - \mathcal{A}^2}{8\xi} - 1 \right) \sin\left(\frac{\mathcal{A}\mathcal{B}}{8\xi}\right) \right] \times \exp\left(-\frac{\mathcal{B}^2 - \mathcal{A}^2}{16\xi} \right) \frac{\mu\,\mathrm{d}\mu}{\sqrt{1-\mu^2}} \tag{48}$$

and

$$\Xi(\xi,t) = -\frac{\Delta'}{4\pi\sqrt{\pi}} \frac{x}{c} \frac{1}{\sqrt{(t-\xi)^2 - x^2/c^2}} \frac{1}{\xi^{3/2}} \int_{-1}^{1} \left[\left(\frac{\mathcal{B}^2 - \mathcal{A}^2}{8\xi} - 1 \right) \cos\left(\frac{\mathcal{A}\mathcal{B}}{8\xi}\right) + \frac{\mathcal{A}\mathcal{B}}{4\xi} \sin\left(\frac{\mathcal{A}\mathcal{B}}{8\xi}\right) \right] \times \exp\left(-\frac{\mathcal{B}^2 - \mathcal{A}^2}{16\xi} \right) \frac{\mu\,\mathrm{d}\mu}{\sqrt{1-\mu^2}}, \tag{49}$$

where

$$\mathcal{A} = \Delta' \mu \sqrt{(t-\xi)^2 - \frac{x^2}{c^2}} \quad \text{and} \quad \mathcal{B} = b'(t-\xi).$$

The Green function is given by

$$G(x,t) = \begin{cases} 0 & \text{if} \quad 0 \le t \le \dfrac{x}{c}, \\ F_1(t) + \int_0^{t - x/c} H(\xi,t)\,\mathrm{d}\xi + i \int_0^{t - x/c} \Xi(\xi,t)\,\mathrm{d}\xi & \text{if} \quad t > \dfrac{x}{c}. \end{cases} \tag{50}$$

4.4. Numerical simulations

Take a sample of plastic foam M1, which is a porous material saturated with air, with the following parameters: thickness 0.8 cm, tortuosity $\alpha_\infty = 1.5$, viscous characteristic length $\Lambda = 25\ \mu\mathrm{m}$, thermal characteristic length $\Lambda' = 75\ \mu\mathrm{m}$, flow resistivity $\sigma = 2\,00\,000\ \mathrm{N\,m^{-4}\,s}$, porosity $\phi = 0.82$ and thermal permeability $k_0' = 2.77 \times 10^{-10}\ \mathrm{m^2}$. Simulated transmitted signal is computed from Eq. (23). The input signal is given in Fig. 1(a) and its spectrum in Fig. 1(b).

Fig. 2(a) shows a comparison between two simulated signals, the first (solid line) corresponds to the real part of the solution (50) when $p = p' = 0.7$ and the second (dashed line) corresponds to the solution (42) calculated in Ref. [13] according to the Johnson–Allard model when $p = p' = 1$. We chose the same values for p and p' to simplify this study. This specified value of 0.7 is valid only for porous material with circular pores [15]. In the

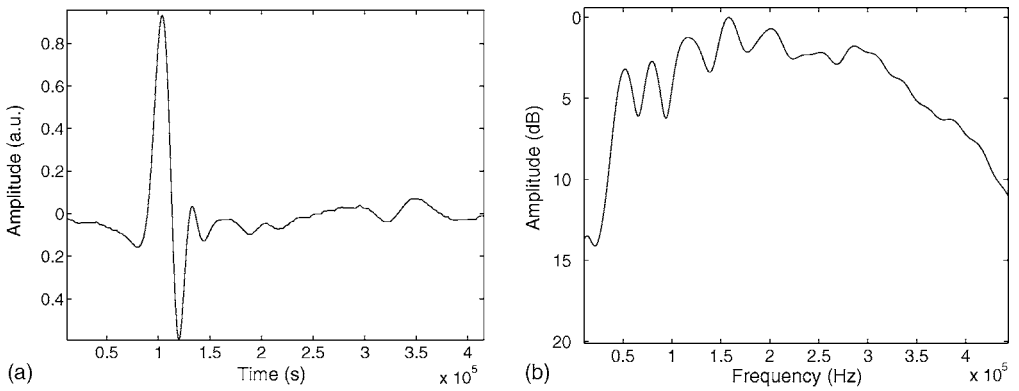

Fig. 1. (a) Input signal; (b) spectrum of the incident signal.

general case, the values of p and p' may be different from 0.7 (see [15]). Note that it is possible to have a positive value of Δ^2 for other values of p and p'.

From Fig. 2(a), we can see that an important change occurs in wave amplitude. By increasing p and p' from 0.7 to 1, wave amplitude increases by 65% of its initial value. This result can be predicted by the fact that when p and p' increase, coefficient C decreases and thus wave attenuation decreases due to inertial, viscous and thermal interactions between fluid and structure. This phenomenon is much more significant for resistive porous materials. Fig. 2(b) shows the same comparison as Fig. 2(a) for another less resistive sample M2, with the following parameters: thickness 0.8 cm, tortuosity $\alpha_\infty = 1.05$, viscous characteristic length $\Lambda = 300\,\mu$m, thermal characteristic length $\Lambda' = 900\,\mu$m, flow resistivity $\sigma = 20\,000\,\mathrm{N\,m^{-4}\,s}$, porosity $\phi = 0.96$ and thermal permeability $k_0' = 2.77 \times 10^{-9}\,\mathrm{m^2}$. In Fig. 2(b), the influence of the parameters p and p' on the attenuation is lower than in Fig. 2(a). We can conclude that the parameters p and p' play an important role in the acoustic attenuation, especially for resistive porous materials.

It can be seen from Fig. 2 that when p and p' changed from 0.7 to 1, the waveform is changed only in attenuation (wave amplitude) and not in dispersion. Fig. 3 shows the spectra of the two simulated signals given in Fig. 2(a). From the spectra of the two simulated signals, it can be seen that they have the same bandwidths which means that there is no dispersion. This end result shows that p and p' play an important role in acoustic wave attenuation but not in dispersion, as is the case for viscous and thermal characteristic lengths [11,12].

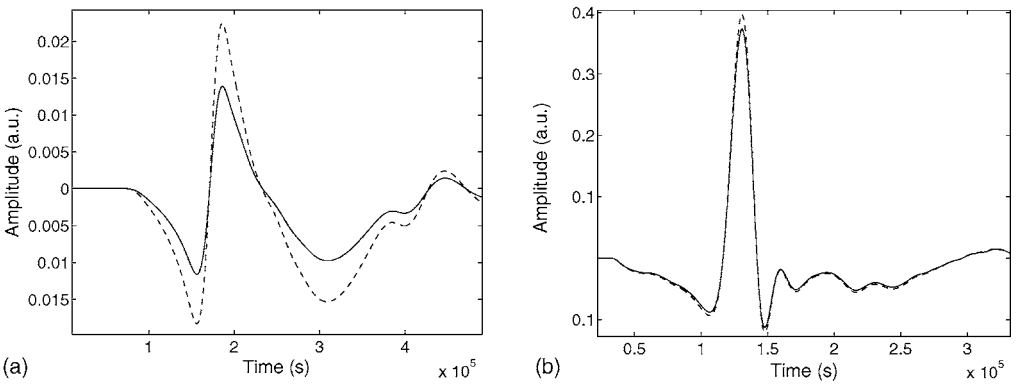

Fig. 2. (a) Comparison between simulated transmitted signal corresponding to the real part of the solution (50) for $p = p' = 0.7$ (solid line), and simulated signal corresponding to solution (42) for $p = p' = 1$ (dashed line), for the sample M1; (b) comparison between simulated transmitted signal corresponding to the real part of the solution (50) for $p = p' = 0.7$ (solid line), and simulated signal corresponding to solution (42) for $p = p' = 1$ (dashed line), for the sample M2.

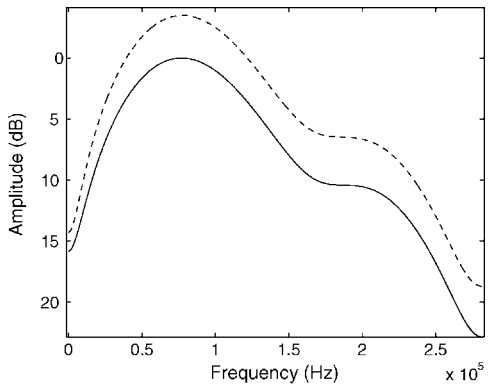

Fig. 3. Spectrum of simulated transmitted signal for $p = p' = 0.7$ (Eq. (50)) (solid line) and spectrum of simulated transmitted signal for $p = p' = 1$ (Eq. (42)) (dashed line).

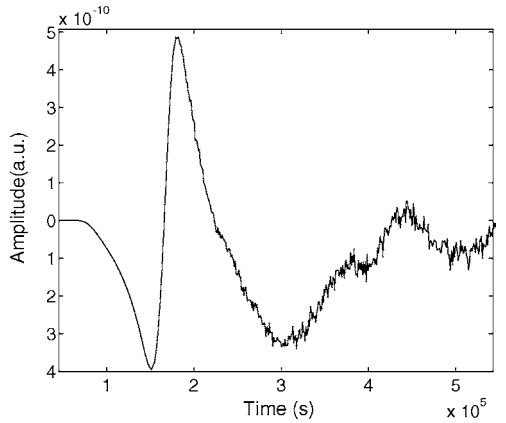

Fig. 4. Simulated transmitted signal corresponding to the imaginary part of the solution (50).

Fig. 4 shows the imaginary part of the solution (50) for $p = p' = 0.7$ (sample M1). The amplitude of the imaginary part of the solution is very small compared to the real part (Fig. 2(a)). This is the reason why only the real part of the solution corresponding to the physical solution is taken into account when a comparison with experiments is made. It is possible to write the complex Green function given in Eq. (50) as $G = G_1 + \mathrm{i}G_2 = |G|\, e^{\mathrm{i}\theta}$, $\tan\theta = G_2/G_1 \ll 1$. This leads to the conclusion that all the signal components get the same (very small) phase θ which is from this fact an inessential physical factor. This means that though the Pride–Lafarge model extends the range of validity of the fluid equivalent model, the Pride's parameters need to be interpreted physically.

In the next section, experimental validation of the solution (50) of the propagation equation for another plastic foam is given.

5. Ultrasonic measurements

As an application of this model, certain numerical simulations are compared to experimental results. Experiments are performed in air using two broadband Panametrics V389 piezoelectric transducers with 250 kHz central frequency in air and a bandwidth at 6 dB OF 60–420 kHz. 900 V pulses are provided by a 5058PR Panametrics

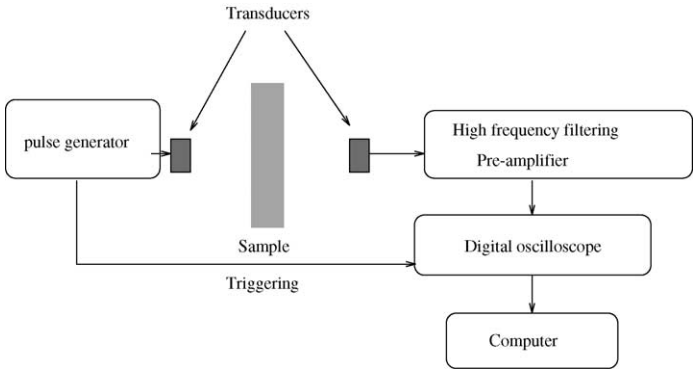

Fig. 5. Experimental set-up of the ultrasonic measurements.

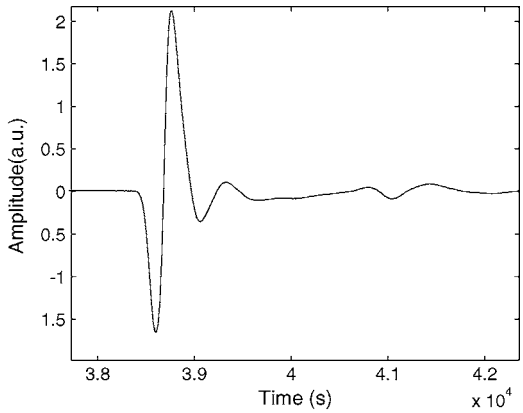

Fig. 6. Experimental incident signal generated by the transducer.

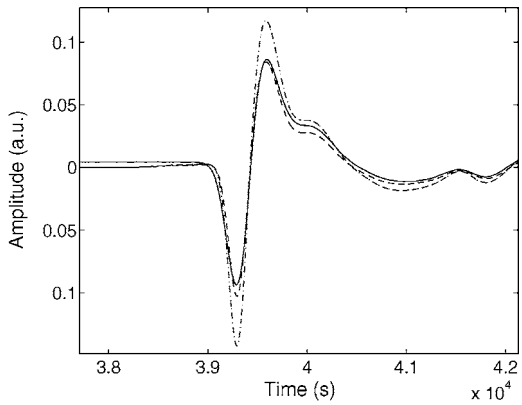

Fig. 7. Experimental transmitted signal (solid line), simulated transmitted signal given by the real part of the Eq. (50) when $p = p' = 0.7$ (dashed line) and the simulated transmitted signal given by the solution (42) when $p = p' = 1$ (dashdot line).

pulser/receiver. The signals received are amplified to 90 dB and filtered above 1 MHz to avoid high frequency noise. (The energy is totally filtered by the sample in this upper frequency domain.) Electronic interference is removed by 1000 acquisition averages. The experimental setup is shown in Fig. 5.

Take a sample of air-saturated plastic foam M3 with the following parameters determined by conventional methods [11,12]: thickness 0.8 cm, tortuosity $\alpha_\infty = 1.5$, viscous characteristic length $\Lambda = 35\,\mu\text{m}$, thermal characteristic length $\Lambda' = 105\,\mu\text{m}$, flow resistivity $\sigma = 125\,000\,\text{N}\,\text{m}^{-4}\,\text{s}$, porosity $\phi = 0.9$ and thermal permeability $k_0' = 4.44 \times 10^{-9}\,\text{m}^2$. Fig. 6 shows the experimental incident signal generated by the transducer. In Fig. 7, we compare the experimental transmitted signal (solid line), the simulated transmitted signal given by the real part of the Eq. (50) when $p = p' = 0.7$ (dashed line) and the simulated transmitted signal given by the solution (42) when $p = p' = 1$ (dashdot line). This comparison shows that the theoretical data obtained by Pride–Lafarge model leads to better results than those given by Johnson–Allard model.

6. Conclusion

In this paper, an analytical solution in the time domain for the propagation of ultrasonic waves in porous media with a rigid frame is established using the Pride–Lafarge model. This model is more general than the Johnson–Allard one which leads to underestimation of the imaginary part of the viscous and thermal relaxation functions. The solution of the propagation equation is solved using the Laplace transform and an experimental validation of the solution of the propagation equation is given. The direct problem is solved by taking into account the two new parameters p and p' introduced by Pride et al. and Lafarge. One important result of this work is that the introduction of the two parameters p and p' corrects the Johnson–Allard model by increasing attenuation with no change in dispersion. This phenomenon is much more significant for resistive porous materials. This analytical solution will help us to improve the characterization of porous material by solving the inverse problem in the time domain. To progress in this area, coming works will must improve the physical interpretation of the Pride–Lafarge parameters.

Appendix A

We use the relation [23]

$$\int_0^\infty \frac{\exp\left(-a\sqrt{x^2+y^2}\right)}{\sqrt{x^2+y^2}} J_0(bx)x\,\mathrm{d}x = \frac{\exp\left(-y\sqrt{a^2+b^2}\right)}{\sqrt{a^2+b^2}}, \quad (a,b) > 0. \tag{A.1}$$

where $J_0(x)$ is the Bessel function, and a, b are constants. By changing the variables $\zeta = \sqrt{x^2+y^2}$, we get

$$\int_y^{+\infty} \exp(-a\zeta) J_0\left(b\sqrt{\zeta^2-y^2}\right)\mathrm{d}\zeta = \frac{\exp\left(-y\sqrt{a^2+b^2}\right)}{\sqrt{a^2+b^2}}. \tag{A.2}$$

By differentiating the two sides of Eq. (A.2) with respect to y, and by using the results

$$J_0(0) = 1 \quad \text{and} \quad \frac{\partial J_0(x)}{\partial x} = -J_1(x), \tag{A.3}$$

we obtain the relation

$$\exp\left(-y\sqrt{a^2+b^2}\right) = \exp(-ay) - by\int_y^{+\infty} \exp(-a\zeta)\frac{J_1\left(b\sqrt{\zeta^2-y^2}\right)}{\sqrt{\zeta^2-y^2}}\,\mathrm{d}\zeta. \tag{A.4}$$

By choosing in Eq. (A.4) the expressions $y = x/c$, $a = z + b'/2\sqrt{z}$ and $b = \Delta'\sqrt{z}/2$, we find that

$$\exp\left(-\frac{x}{c}\sqrt{f(z)}\right) = \exp\left(-\left(z + \frac{b'}{2}\sqrt{z}\right)\frac{x}{c}\right) - \frac{\Delta'\sqrt{z}}{2}\frac{x}{c}\int_{x/c}^{+\infty} \exp\left(-\left(z + \frac{b'}{2}\sqrt{z}\right)\zeta\right) \times \frac{J_1\left(\Delta'\sqrt{z}/2\sqrt{\zeta^2 - x^2/c^2}\right)}{\sqrt{\zeta^2 - x^2/c^2}}\,\mathrm{d}\zeta. \tag{A.5}$$

The first term in the right-hand side of Eq. (A.5) was calculated in Ref. [13]

$$\mathcal{L}^{-1}\left[\exp -\frac{x}{c}\left(z + \frac{b'}{2}\sqrt{z}\right)\right] = \frac{1}{4\sqrt{\pi}}\frac{b'x}{c}\frac{1}{(t - x/c)^{3/2}}\exp\left[-\frac{b'^2x^2}{16c^2(t - x/c)}\right]. \tag{A.6}$$

It should be remembered that an integral representation of the Bessel function $J_1(z)$ is [21]

$$J_1(z) = \frac{z}{\pi}\int_{-1}^{1} \exp(\mathrm{i}zt)\sqrt{1 - t^2}\,\mathrm{d}t, \tag{A.7}$$

By substituting $\wp z$ in place of z, we obtain

$$J_1(\wp z) = \frac{\wp z}{\pi}\int_{-1}^{1} \exp(\mathrm{i}\wp zt)\sqrt{1 - t^2}\,\mathrm{d}t, \tag{A.8}$$

which, with the variable change $T = -\mathrm{i}\wp t$, yields

$$J_1(\wp z) = -\frac{\mathrm{i}z}{\pi}\int_{-\mathrm{i}\wp}^{\mathrm{i}\wp} \exp(-zT)\sqrt{1 + \frac{T^2}{\wp^2}}\,\mathrm{d}T. \tag{A.9}$$

we then have

$$\mathcal{L}^{-1}[J_1(\wp z)] = \frac{\mathrm{d}}{\mathrm{d}t}\left(-\frac{\mathrm{i}}{\pi}\sqrt{1 + \frac{t^2}{\wp^2}}\right) \quad \text{for } -\mathrm{i}\wp \le t \le \mathrm{i}\wp, \tag{A.10}$$

which means that

$$\mathcal{L}^{-1}[J_1(\wp z)] = -\frac{\mathrm{i}}{\pi}\frac{1}{\wp^2}\frac{t}{\sqrt{1 + t^2/\wp^2}} \quad \text{for } -\mathrm{i}\wp \le t \le \mathrm{i}\wp. \tag{A.11}$$

We then deduce the following relation

$$\mathcal{L}^{-1}\left[\exp\left(-\frac{b'}{2}\zeta z\right)J_1(\wp z)\right] = -\frac{\mathrm{i}}{\pi}\frac{1}{\wp^2}\frac{t - \zeta b'/2}{\sqrt{1 + (t - \eta b'/2)^2/\wp^2}} \quad \text{for } -\mathrm{i}\wp \le t - \frac{b'}{2}\zeta \le \mathrm{i}\wp, \tag{A.12}$$

which gives (Appendix B)

$$\mathcal{L}^{-1}\left[\sqrt{z}\exp\left(-\frac{b'}{2}\zeta\sqrt{z}\right)J_1(\wp\sqrt{z})\right] = \frac{-\mathrm{i}}{2\pi\sqrt{\pi}}\frac{1}{\wp^2}\frac{1}{t^{3/2}}\int_{b'/2\zeta - \mathrm{i}\wp}^{b'/2\zeta + \mathrm{i}\wp} \exp\left(-\frac{u^2}{4t}\right)\left(\frac{u^2}{2t} - 1\right)\frac{u - \zeta b'/2}{\sqrt{1 + (u - \zeta b'/2)^2/\wp^2}}\,\mathrm{d}u. \tag{A.13}$$

By changing the variables in Eq. (A.13)

$$\mu = \frac{u - \zeta b'/2}{\mathrm{i}\wp} \Rightarrow \mathrm{d}u = \mathrm{i}\wp\,\mathrm{d}\mu,$$

we then obtain

$$\mathcal{L}^{-1}[\sqrt{z}\exp(-\zeta\sqrt{z}b'/2)J_1(\wp\sqrt{z})] = \frac{\mathrm{i}}{2\pi\sqrt{\pi}}\frac{1}{t^{3/2}}\int_{-1}^{1}\exp-\left(\frac{(\mathrm{i}\wp\mu+\zeta b'/2)^2}{4t}\right)\left[\frac{(\mathrm{i}\wp\mu+\zeta b'/2)^2}{2t}-1\right]\frac{\mu\,\mathrm{d}\mu}{\sqrt{1-\mu^2}}. \tag{A.14}$$

It follows from Eq. (A.14) that

$$\mathcal{L}^{-1}[\sqrt{z}\exp(-\zeta(z+\sqrt{z}b'/2))J_1(\wp\sqrt{z})] = \frac{\mathrm{i}}{2\pi\sqrt{\pi}}\frac{1}{(t-\zeta)^{3/2}}\int_{-1}^{1}\exp\left(-\frac{(\mathrm{i}\wp\mu+\zeta b'/2)^2}{4(t-\zeta)}\right)\left[\frac{(\mathrm{i}\wp\mu+\zeta b'/2)^2}{2(t-\zeta)}-1\right]\frac{\mu\,\mathrm{d}\mu}{\sqrt{1-\mu^2}}, \quad t\geq\zeta\geq\frac{x}{c}. \tag{A.15}$$

We then choose $\wp$ such that

$$\wp=\wp(\zeta)=\frac{\Delta'}{2}\sqrt{\zeta^2-\frac{x^2}{c^2}}. \tag{A.16}$$

Consequently, Eq. (A.15) becomes

$$\begin{aligned}\mathcal{L}^{-1}&\left[\sqrt{z}\exp\left(-\zeta\left(z+\frac{\sqrt{z}b'}{2}\right)\right)\frac{J_1[\Delta'/2\sqrt{z}\sqrt{\zeta^2-x^2/c^2}]}{\sqrt{\zeta^2-x^2/c^2}}\right]\\ &=\frac{\mathrm{i}}{2\pi\sqrt{\pi}}\frac{1}{\sqrt{\zeta^2-x^2/c^2}}\frac{1}{(t-\zeta)^{3/2}}\int_{-1}^{1}\exp\left(-\frac{(\mathrm{i}\Delta'\mu\sqrt{\zeta^2-x^2/c^2}+\zeta b')^2}{16(t-\zeta)}\right)\\ &\quad\times\left[\frac{(\mathrm{i}\Delta'\mu\sqrt{\zeta^2-x^2/c^2}+b'\zeta)^2}{8(t-\zeta)}-1\right]\frac{\mu\,\mathrm{d}\mu}{\sqrt{1-\mu^2}}.\end{aligned} \tag{A.17}$$

We can now calculate the inverse Laplace transform of Eq. (A.5)

$$\begin{aligned}\mathcal{L}^{-1}\left[\exp\left(-\frac{x}{c}\sqrt{f(z)}\right)\right]=&-\frac{i\Delta'}{4\pi\sqrt{\pi}}\frac{x}{c}\int_{x/c}^{t}\frac{1}{\sqrt{\zeta^2-x^2/c^2}}\frac{1}{(t-\zeta)^{3/2}}\int_{-1}^{1}\exp\left(-\frac{(\mathrm{i}\Delta'\mu\sqrt{\zeta^2-x^2/c^2}+\zeta b')^2}{16(t-\zeta)}\right)\\ &\times\left[\frac{(\mathrm{i}\Delta'\mu\sqrt{\zeta^2-x^2/c^2}+\zeta b')^2}{8(t-\zeta)}-1\right]\frac{\mu\,\mathrm{d}\mu}{\sqrt{1-\mu^2}}.\end{aligned} \tag{A.18}$$

Using the variable change $t-\zeta=\xi$, we obtain

$$\mathcal{L}^{-1}\left[\exp\left(-\frac{x}{c}\sqrt{f(z)}\right)\right]=\int_0^{t-x/c}h(\xi,t)\,\mathrm{d}\xi,$$

with

$$\begin{aligned}h(\xi,\tau)=&-\frac{\mathrm{i}\Delta'}{4\pi\sqrt{\pi}}\frac{x}{c}\frac{1}{\sqrt{(t-\xi)^2-x^2/c^2}}\frac{1}{\xi^{3/2}}\int_{-1}^{1}\exp\left(-\frac{(\mathrm{i}\Delta'\mu\sqrt{(t-\xi)^2-x^2/c^2}+b'(t-\xi))^2}{16\xi}\right)\\ &\times\left[\frac{(\mathrm{i}\Delta'\mu\sqrt{(t-\xi)^2-x^2/c^2}+b'(t-\xi))^2}{8\xi}\right]\frac{\mu\,\mathrm{d}\mu}{\sqrt{1-\mu^2}}.\end{aligned}$$

By separating the real and imaginary part of the function $h(\xi, t)$, we then obtain

$$h(\xi, t) = H(\xi, t) + i\Xi(\xi, t).$$

Appendix B

If $f(u)$ is the inverse Laplace transform of a function $g(z)$

$$g(z) = \int_0^\infty \exp(-zu)\, f(u)\, \mathrm{d}u. \tag{B.1}$$

The inverse Laplace transform of $\sqrt{z}g(z)$ is

$$\mathcal{L}^{-1}(\sqrt{z}g(z)) = \frac{1}{2\sqrt{\pi}}\frac{1}{t^{3/2}}\int_0^\infty \left(\frac{u^2}{2t} - 1\right)\exp\left(-\frac{u^2}{4t}\right) f(u)\, \mathrm{d}u. \tag{B.2}$$

In our case

$$g(z) = \exp\left(-z\frac{b'}{2}\xi\right) J_1(\wp z) \tag{B.3}$$

and

$$f(u) = -\frac{\mathrm{i}}{\pi}\frac{1}{\wp^2}\frac{u - \xi b'/2}{\sqrt{1 + (u - \xi b'/2)^2/\wp^2}}, \qquad -\mathrm{i}\wp \le u - \frac{\xi b'}{2} \le \mathrm{i}\wp. \tag{B.4}$$

which give us the relation (A.13).

References

[1] G. Krichhoff, Uber der Einfluss Wärmeleitung in einem Gase auf die Schallbewegung, Annalen der Physik and Chemie. 134 (1868) 177–193.
[2] C. Zwikker, C.W. Kosten, Sound Absorbing Materials, Elsevier, New York, 1949.
[3] H. Tijdeman, On the propagation of sound waves in cylindrical tubes, J. Sound Vib. 39 (1975) 1–33.
[4] M.R. Stinson, The propagation of plane sound waves in narrow and wide circular tubes, and generalization to uniform tubes of arbitrary cross-sectional shape, J. Acoust. Soc. Am. 89 (1991) 550–558.
[5] K. Attenborough, Acoustical characteristics of porous materials, Phys. Rep. 82 (1982) 179–227.
[6] R.F. Lambert, Propagation of sound in highly porous open cells elastic foams, J. Acoust. Soc. Am. 73 (1983) 1131–1138.
[7] K. Attenborough, On the acoustic slow wave in air-filled granular media, J. Acoust. Soc. Am. 81 (1987) 93–102.
[8] D.L. Johnson, J. Koplik, R. Dashen, Theory of dynamic permeability and tortuosity in fluid-saturated porous media, J. Fluid Mech. 176 (1987) 379–402.
[9] J.F. Allard, Propagation of Sound in Porous Media: Modeling Sound Absorbing Materials, Chapman and Hall, London, 1993.
[10] Y. Champoux, J.F. Allard, Dynamic tortuosity and bulk modulus in air-saturated porous media, J. Appl. Phys. 70 (4) (1991) 1975–1979.
[11] Z.E.A. Fellah, C. Depollier, Transient acoustic wave propagation in rigid porous media: a time-domain approach, J. Acoust. Soc. Am. 107 (2000) 683–688.
[12] Z.E.A. Fellah, M. Fellah, W. Lauriks, C. Depollier, Direct and inverse scattering of transient acoustic waves by a slab of rigid porous material, J. Acoust. Soc. Am. 113 (2003) 61–73.
[13] Z.E.A. Fellah, M. Fellah, W. Lauriks, C. Depollier, J.Y. Chapelon, Y.C. Angel, Solution in time domain of ultrasonic propagation equation in a porous material, Wave Motion 38 (2003) 151–163.
[14] D. Lafarge, P. Lemarnier, J.F. Allard, V. Tarnow, Dynamic compressibility of air in porous structures at audible frequencies, J. Acoust. Soc. Am. 102 (1997) 1995–2006.
[15] D. Lafarge, Sound propagation in porous materials having a rigid frame saturated by gas, (in French). Ph.D. Dissertation, Université du Maine, 1993.
[16] T.L. Szabo, Time domain wave equations for lossy media obeying a frequency power law, J. Acoust. Soc. Am. 96 (1994) 491–500.
[17] S.R. Pride, F.D. Morgan, A.F. Gangi, Drag forces of a porous-medium acoustics, Phys. Rev. B (1993) 4964–4978.

[18] M.A. Biot, The theory of propagation of elastic waves in fluid-saturated porous solid. I. Low frequency range, J. Acoust. Soc. Am. 28 (1956) 168–178.
[19] M.A. Biot, The theory of propagation of elastic waves in fluid-saturated porous solid. I. Higher frequency range, J. Acoust. Soc. Am. 28 (1956) 179–191.
[20] S.G. Samko, A.A. Kilbas, O.I. Marichev, Fractional Integrals and Derivatives: Theory and Applications, Gordon and Breach Science Publishers, Amsterdam, 1993.
[21] I. Podlubny, Fractional Differential Equations, Academic Press, San Diego, 1999.
[22] R. Hilfer (Ed.), Applications of Fractional Calculus in Physics, World Scientific, 2000.
[23] I.S. Gradshteyn, I.M. Ryzhik, Table of Integrals, Series and Products, 4th ed., Academic Press, New York, 1965.